

Original Article

Establishment of genetically diverse patient-derived xenografts of colorectal cancer

Danielle M Burgenske^{1,2}, David J Monsma³, Dawna Dylewski³, Stephanie B Scott³, Aaron D Sayfie¹, Donald G Kim⁴, Martin Luchtefeld⁴, Katie R Martin¹, Paul Stephenson⁵, Galen Hostetter⁶, Nadav Dujovny⁴, Jeffrey P MacKeigan^{1,2}

¹Laboratory of Systems Biology, Van Andel Research Institute, Grand Rapids, MI 49503, USA; ²Van Andel Institute Graduate School, Grand Rapids, MI 49503, USA; ³Preclinical Therapeutics, Van Andel Research Institute, Grand Rapids, MI 49503, USA; ⁴Ferguson-Blodgett Digestive Disease Institute, Spectrum Health Medical Group, Grand Rapids, MI 49503, USA; ⁵Department of Statistics, Grand Valley State University, Allendale, MI 49401, USA; ⁶Laboratory of Analytical Pathology, Van Andel Research Institute, Grand Rapids, MI 49503, USA

Received September 10, 2014; Accepted October 20, 2014; Epub November 19, 2014; Published November 30, 2014

Abstract: Preclinical compounds tested in animal models often show limited efficacy when transitioned into human clinical trials. As a result, many patients are stratified into treatment regimens that have little impact on their disease. In order to create preclinical models that can more accurately predict tumor responses, we established patient-derived xenograft (PDX) models of colorectal cancer (CRC). Surgically resected tumor specimens from colorectal cancer patients were implanted subcutaneously into athymic nude mice. Following successful establishment, fourteen models underwent further evaluation to determine whether these models exhibit heterogeneity, both at the cellular and genetic level. Histological review revealed properties not found in CRC cell lines, most notably in overall architecture (predominantly columnar epithelium with evidence of gland formation) and the presence of mucin-producing cells. Custom CRC gene panels identified somatic driver mutations in each model, and therapeutic efficacy studies in tumor-bearing mice were designed to determine how models with known mutations respond to PI3K, mTOR, or MAPK inhibitors. Interestingly, MAPK pathway inhibition drove tumor responses across most models tested. Noteworthy, the MAPK inhibitor PD0325901 alone did not significantly mediate tumor response in the context of a KRAS^{G12D} model, and improved tumor responses resulted when combined with mTOR inhibition. As a result, these genetically diverse models represent a valuable resource for preclinical efficacy and drug discovery studies.

Keywords: Targeted therapies, translational models, colorectal cancer, patient-derived xenograft, AZD8055, BEZ235, PD0325901

Introduction

Transitioning basic research findings into clinical advances has historically posed significant challenges, notably within the oncology field. While many anticancer therapeutics show favorable tumor responses in preclinical models, 95% of these preclinical compounds fail to perform better than standard of care when transitioned into human trials [1]. These outcomes highlight the growing need for reliable preclinical models capable of accurately predicting therapeutic efficacy. Currently, the most common preclinical model is the subcutaneous cell line xenograft (XG) model, which relies on the propagation of well characterized human tumor cell lines in immunocompromised mice. While this approach allows many models to be

established with relative ease, the two-dimensional culturing has profound effects on overall gene expression, tumor heterogeneity, and other cellular properties [2-4]. As a result, these cell lines exhibit little resemblance to the original parental tumors; a feature which greatly limits the relevance of these models.

To address this significant problem, patient-derived xenograft (PDX) models have recently been developed. By direct use of surgically resected human tumor specimens, a larger percentage of the parental tumor's heterogeneity is retained [5-7]. The composition of these tumors extends beyond the tumor bed to include critical stromal elements, which provide sustenance under periods of extensive growth. With the inclusion of support cells in the micro-

environment, the PDX tumors more closely recapitulate the carcinomas from which they are derived; and by extension, provide a more predictive experimental model for evaluating therapeutic responses.

The National Cancer Institute (NCI) sponsored Pediatric Preclinical Testing Program (PPTP) was one of the first efforts that has demonstrated the accuracy and utility of PDX models. The PPTP tested 75 PDX models to prioritize the transition of promising adult anticancer therapies from Phase I trials into a pediatric context [8, 9]. As a proof of principle, this work demonstrated that PDX models could mimic clinical responses when tested in a relevant disease context [9]. Furthermore, patients could be prospectively assigned to treatment strategies as a result of these preclinical compound studies [10].

Given the initial successes using PDX models, an important focus is to develop models for diseases where ineffective treatments exist. While many compounds have documented success in traditional preclinical models, efficacy is often lost when administered to cancer patients [11]. These inconsistencies underscore an unmet clinical need for more accurate models. Improving the spectrum of available preclinical models will significantly aid in combating current limitations of primary therapies.

As the second leading cause of cancer related deaths in the United States, CRC remains a substantial clinical problem. The American Cancer Society (ACS) projects 136,830 Americans to be diagnosed with CRC in 2014 [12]. While five-year survival rates remain high for patients diagnosed in the early stages of disease, a stage IV diagnosis reduces survival to below 10% [13]. More recently, molecularly targeted therapies are becoming standard of care for advanced CRC. Components of growth factor signaling, mainly vascular endothelial growth factor (VEGF) and epidermal growth factor receptor (EGFR), have been tested and approved [14, 15]. These inhibitors have been met with mixed results as only subsets of patients appear to benefit [15, 16]. A patient population of specific concern is those patients with KRAS mutations, as they exhibit drug resistance to most therapeutics [17-20]. The Ras family of small GTPases consists of three main members (KRAS, HRAS, and NRAS), which execute several cellular functions including pro-

liferation, differentiation and survival [21, 22]. Diverse extracellular stimuli are capable of initiating this signal transduction cascade, most notably the EGFR [22].

Constitutive Ras activation is found in up to one-third of all cancer types, with dysregulation resulting in activated downstream signaling cascades, including the PI3K and MAPK pathways [23, 24]. Given the intractability of Ras as a therapeutic target, PI3K and MAPK signaling inhibition present promising alternatives to inhibit downstream targets [25-27]. In this study, we establish and characterize CRC PDX models in a concerted effort to provide more representative disease models. We evaluated the dual PI3K/mTOR inhibitor, BEZ235; the mTOR inhibitor, AZD8055; and the MEK inhibitor, PD0325901, as single agents and in combinations. While cell line xenografts have been used to test molecularly targeted agents in other disease contexts, the performance of these specific regimens has yet to be collectively assessed with CRC PDX models [28-42].

Materials and methods

Patient tumor tissue

This study was approved by the Institutional Review Boards of Van Andel Institute and Spectrum Health Hospitals (Grand Rapids, MI). Written informed consent was obtained from all patients prior to enrollment with participation being contingent on two clinical parameters: patient 1) had confirmed or highly suspected primary colorectal cancer, and 2) was scheduled for surgical resection at Spectrum Health Hospital. All resected tumor specimens underwent evaluation by a board-certified Spectrum Health Hospital pathologist. Based on final histopathological staging, patients were stratified into the appropriate clinical regimens. Following completion of these regimens, patients reported back yearly for clinical evaluation.

PDX cohort expansion

Athymic nude mice from the Van Andel Research Institute internal breeding colony were used in this study. All animal studies were handled in accordance with the guidelines provided by the Van Andel Institutional Animal Care and Use Committee (IACUC) with food and water available *ad libitum*. Patient-derived xenograft models were established by propa-

gating patient specimens subcutaneously into the flank of gender matched athymic nude mice (described below). Mice were euthanized and tumors harvested in accordance with IACUC guidelines.

Establishment of PDX models

Tumor specimens were placed into transfer media [RPMI 1640 media (Invitrogen, Carlsbad CA), 10% fetal bovine serum (Mediatech, Manassas, VA), 1% penicillin/streptomycin (Invitrogen), and 50 units/mL Heparin (Sigma, St. Louis, MO)] and delivered to Van Andel Institute on ice within 30 minutes of resection. Tumor specimens were moved into individual petri dishes of sterile phosphate buffered saline (Invitrogen) and separated into ≤ 3 mm fragments within one hour of receipt. Depending on the size of the specimen, up to five gender matched athymic nude mice were used for tumor propagation. Each mouse was treated with the analgesic ketoprofen (5 mg/kg body weight) with betadine (Purdue Products LP, Stamford, CT) being used to sterilize the right flank prior to surgery. While under isoflurane anesthesia, a subcutaneous pocket was subsequently created and the tumor fragment was inserted prior to closing with surgical staples. Postoperative care included daily animal monitoring for overall health and tumor growth. Tumor volumes were measured by calipers in three dimensions and calculated using the following equation: ($\frac{1}{2}$ x length x depth x height). Measurements were taken once weekly when tumor volumes ≤ 100 mm³ and three times weekly when > 100 mm³. In parallel with these measurements, weekly body weights were also recorded. Animals were maintained until tumor burden euthanasia criterion was met (tumor volume of ~ 1500 mm³); at which point, mice were euthanized and tumors were aseptically harvested. The resected tumors from this group (denoted as the F0 generation) were then subdivided to allot material for both cryopreservation and subsequent propagation *in vivo*. Propagated fragments maintained dimensions below 3 mm in size and were conducted as stated above.

Histologic evaluation

Harvested tumors were immediately placed in 10% formalin (Azer Scientific, Morgantown, PA) for 48 to 72 hours before being transferred into

70% ethanol. Specimens were submitted to the Van Andel Research Institute histopathology core for immunohistochemistry using the Ventana Discovery XT immunostainer (Ventana Medical Systems, Tucson, Arizona). Samples were paraffin embedded and sectioned into 5 μ m slices. Serial sections were stained with primary antibodies against pERK-Y202/204 (Cell Signaling Technologies (CST, Danvers, MA) 4376; 1:300), pS6-S240/244 (CST 2215; 1:200), and Ki67 (AbCam (Cambridge, MA) 833; 1:100), for 1 hour at the indicated dilutions. UltraMap anti-Rabbit DAB (3, 3'-diaminobenzidine) detection was followed by incubation with the counterstain hematoxylin (Ventana Medical Systems).

Mutational analysis of tumor DNA

Liquid nitrogen preserved murine tumor specimens were mechanically dissociated and genomic DNA was subsequently isolated using the QIAamp DNA mini kit (Qiagen, Valencia, CA). Purity was determined by spectrophotometry with the A260/A280 ratios > 1.7 . Amplification-refractory mutation (ARM) designed primers against commonly mutated genes in colorectal cancer were ordered from Qiagen (catalog #SMH-021ARA) and used according to manufacturer's instructions. Using an Applied Biosystems 7500 real-time polymerase chain reaction (qRT-PCR) platform, the following protocol conditions were followed: a single DNA polymerase activation cycle at 95°C for 10 minutes followed by 40 two-step anneal and extension cycles (95°C for 15 seconds, 60°C for 1 minute).

Preclinical studies

F1 generation tumors of equivalent size (approximately 3 mm in diameter) from two donor mice were implanted and monitored, as described above, into gender-matched athymic nude mice. Once tumor volumes reached 400 mm³, animals were randomly assigned into the following treatment arms: vehicle (1% carboxymethyl cellulose), AZD8055 (20 mg/kg body weight), BEZ235 (40 mg/kg body weight), PD0325901 (20 mg/kg body weight), AZD8055 + PD0325901 (20 mg/kg of each compound), or BEZ235 + PD0325901 (40 mg/kg and 20 mg/kg, respectively). All drug regimens were administered daily by oral gavage for five consecutive days followed by two days off. Animals

Table 1. Summary of patient demographics

Model ID	Gender	Age	Histopathological Grade	Recurrence
CRC02	F	77	pT3, pN1, pMX	--
CRC06	F	79	pT4, pN1, pMX	Year 1
CRC09	F	49	pT4, pN2, pMX	--
CRC10	F	80	pT3, pN0, pMX	--
CRC12	F	75	pT3, pN0, pMX	--
CRC14	F	52	pT3, pN2, pM0	--
CRC17	F	61	pT3, pN0, pMX	Year 2
CRC18	F	82	pT1, pN0, pMX	--
CRC19	F	70	pT4, pN2, pM1	Year 2
REC02	M	66	pT3, pN0, pMX	Year 2
REC09	F	83	pT3, pN1, pM0	**
REC12	F	41	pT2, pN0, pM1	Year 1
REC16	M	72	pT1, pN0, pMX	--
REC19	M	74	pT3, pN1, pMX	--

Abbreviations: T, tumor staging; N, degree of spread to regional lymph nodes; M, presence of distant metastasis; X, undetermined. **Unknown; no follow-up records available.

Calculation of proliferation indices

Representative Ki67 stained sections from each treatment group were scanned using the Aperio ScanScope CS and associated software ImageScope (Buffalo Grove, IL) for calculation of proliferative indices. Six representative 100x magnification fields were selected and captured in blinded fashion from each slide by a certified pathologist. Total nuclei were counted, and two scorers counted and scored positively stained tumor nuclei. Combined proliferation index (% of Ki67⁺ tumor nuclei/total tumor nuclei) was calculated, and selected fields were tabulated for each group. A proliferation index of 15% or above was designated as highly proliferative [23-26].

Statistical analysis

were continually monitored for changes in tumor volume, overall health, and body weight throughout the study. This regimen was continued for a total of 21 days at which point all remaining animals were euthanatized and the tumor tissue was divided for snap freezing and fixation. Percent change was calculated for all experimental groups using the following formula: [(Day 21 tumor volume - Day 0 tumor volume)/Day 0 tumor volume x 100]. The percent change in the experimental groups was then compared to the vehicle control using the following equation: [(Overall percent change experimental-overall percent change vehicle)/overall percent change vehicle x 100].

Molecularly targeted therapeutics

AZD8055 is an inhibitor of mammalian target of rapamycin (mTOR) kinase with high selectivity [32]. BEZ235 targets the phosphoinositide 3-kinase (PI3K) and mTORC1/mTORC2 complexes [35]. PD0325901 selectively inactivates the mitogen-activated protein kinase kinase (MAPK/ERK kinase or MEK) [43]. AZD8055 and BEZ235 were purchased from Selleck Chemicals (Houston, TX), while PD0325901 was purchased from LC Laboratories (Woburn, MA). All compounds were directly diluted in aqueous 1% carboxymethyl cellulose solution (Sigma, St. Louis, MO) and administered orally via gavage in 100 µL volumes.

Tumor volumes were analyzed employing a repeated measures ANOVA model using SAS (Statistical Analysis Software) 9.3 (SAS Institute Inc., Cary, NC). SAS's PROC MIXED was used to fit a linear mixed model to examine the varying treatment effects over time on tumor volume data, with a random effect accounting for mouse-specific variation. Relevant 95% confidence intervals were constructed using the LSMEANS statement to determine the treatment effectiveness on tumor volume over time. Significance was defined as follows: *p < 0.05, **p < 0.01, and ***p < 0.001.

Results

Establishment of CRC PDX models

Sixteen CRC PDX models were successfully engrafted using subcutaneous transplantation as described above. Patient demographic information for these established xenografts can be found in **Table 1**. All specimens that had successful initial transplants into mice had successful propagation into subsequent mice. To be classified as a successful engraftment, models had to exhibit entry into log growth within six months for two distinct experimental criteria: 1) upon transplant of human tumor into the donor mouse, and 2) upon transplant of a cryopreserved tumor fragment into the recipient. While these specimens reflected a range of histological stages, no obvious correlations

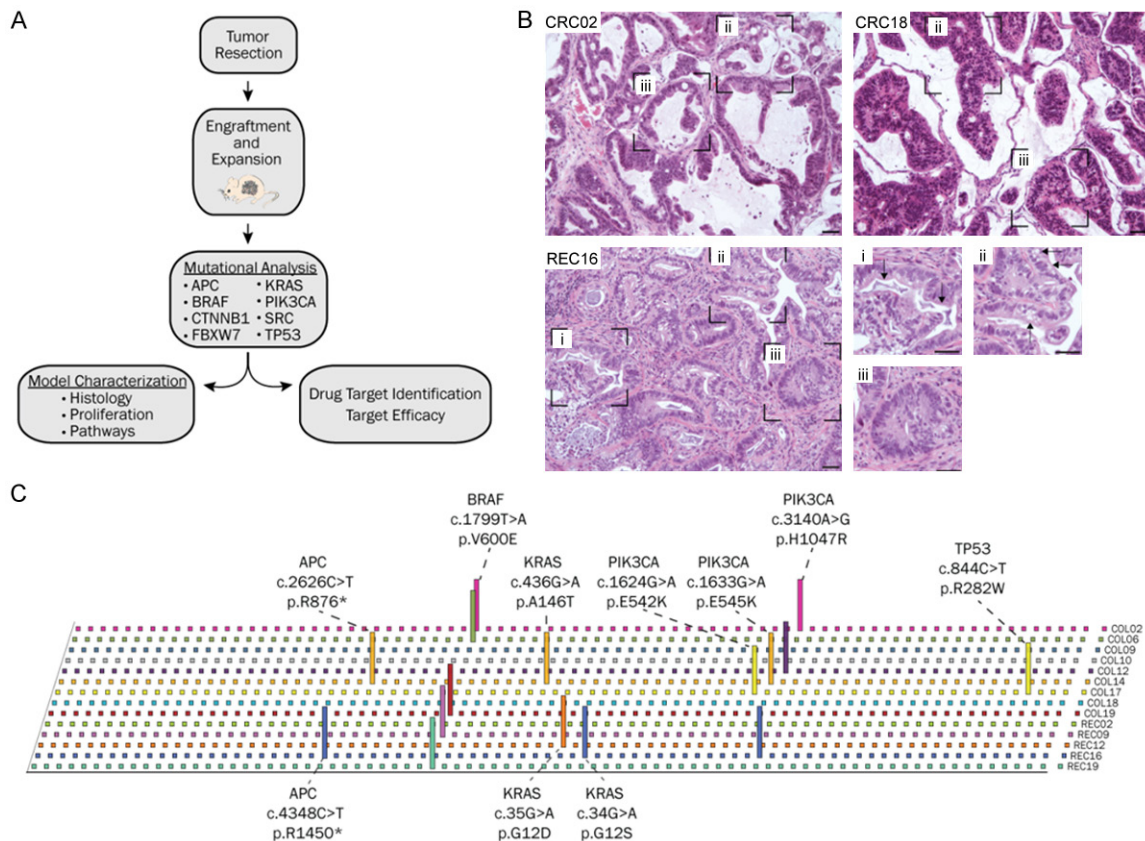


Figure 1. PDX model characterization. **A.** Schematic representation of workflow in PDX establishment. **B.** Representative H&E images from randomly selected models illustrated clinical hallmarks of colorectal cancer. These included evidence of gland formation (i), mucin producing cells (ii), and columnar epithelium (iii). Scale bars indicate 50 μ m. **C.** Using isolated tumor DNA from all models, eighty-five mutations (x axis) were profiled on the somatic mutation PCR panels directed against common mutations in *APC*, *BRAF*, *CTNNB1*, *FBXW7*, *KRAS*, *PIK3CA*, *SRC*, and *TP53*. Each detected mutation is indicated as a peak along with gene symbol, coding change, and mutation.

between successful propagation and tumor grade were observed. This provided the framework for the workflow diagrammed in **Figure 1A**.

Characterization of CRC PDX models

Tumors were excised and subsequently utilized to determine the histological and genomic profile of each model. Hematoxylin and eosin (H&E) stained sections were observed for overall morphology. Across three randomly selected models, hallmarks of clinical colorectal adenocarcinoma were observed (**Figure 1B**). More specifically, these features included gland formation (subpanels i), mucin-producing cells (subpanels ii), and the presence of columnar nuclei with luminal orientation (subpanels iii). Evidence also suggested an active stromal compartment. These features represent clinically

noted attributes of CRC conserved upon transition from a human to murine host.

Following establishment of these models, we initiated an exploratory drug study to identify signaling nodes that may be of clinical value. Appropriate models were selected using custom somatic mutation gene panels. These results highlighted the PI3K and RAS signaling axes as most prevalent across the PDX models (**Figure 1C**). Identified variants were restricted to a set of five genes: *APC*, *BRAF*, *KRAS*, *PIK3CA*, and *TP53*, all of which occur with some frequency in CRC (**Table 2**). Within these models, the most frequently observed mutations were *BRAF*^{V600E} and *PIK3CA*^{H1047R}. These alterations are known oncogenic drivers and dramatically elevate the catalytic activity of both kinases thereby promoting constitutive activation of downstream pathways (e.g. MAPK and mTOR).

Table 2. Genetic alterations in CRC

Gene	Clinically Reported Incidence ¹	PDX Model Identified Variants
APC	70-80%	R875*, R1450*
BRAF	5-10%	V600E
KRAS	40%	A146T, G12D, G12S
PIK3CA	15-25%	E542K, E545K, H1047R
TP53	60-70%	R282W

Abbreviation: *, truncation. Citation: ¹Fearon ER: Molecular genetics of colorectal cancer. *Annu Rev Pathol* 2011, 6: 479-507.

KRAS mutations were also documented, most of which occurred at known hotspot regions in codon 12 [44]. While alterations to APC were less frequent, all observed APC variants were associated with truncation events as is common in humans with APC mutations [44]. Finally, the incidence of TP53 alterations represented the most infrequent mutation within these models. Despite the vast genomic heterogeneity within CRC, the mutations detected within these PDX models overlapped with common mutations found in patients, making these models well suited for therapeutic efficacy tests. Additionally, these mutational profiles provide preclinical CRC models for which PI3K, mTOR, and MAPK pathway inhibition is relevant.

CRC PDX preliminary drug efficacy studies

Following review of the mutational data, three individual models (COL02, COL18, and REC12) were selected for subsequent enrollment in a drug treatment study to investigate the effects of PI3K, mTOR, and/or MAPK pathway inhibition. Models were selected for varying levels of genetic complexity to best examine subtleties in drug efficacy when distinct signaling pathways become dysregulated. COL18 had no detectable mutations, while COL02 had mutations to both BRAF (V600E) and PIK3CA (H1047R), and REC12 possessed a single mutation to KRAS (G12D). This genomic information was integrated with Kyoto Encyclopedia of Genes and Genomes (KEGG) to formulate pathway-specific treatment strategies (Table 3). Treatments consisted of an ATP-competitive mTOR inhibitor (AZD8055), a dual PI3K/mTOR inhibitor (BEZ235), or a MEK inhibitor (PD0325901). In addition, we evaluated combination mTOR/MEK (AZD8055 + PD0325901) and PI3K/mTOR/MEK inhibition (BE-2235 + PD0325901). Drug dosing regimens were

established from laboratory knowledge and a thorough search of previously published work, and administered as indicated in Table 4 [45-48].

As shown in Figure 2A, 2B, COL02 and COL18 exhibited little to moderate reductions in tumor growth with single agents targeted against mTOR and PI3K. In fact, inhibition of mTOR

signaling with AZD8055 had a more pronounced effect on slowing tumor growth than did combined PI3K/mTOR inhibition with BEZ235. Treatment of these same models with the MEK inhibitor, PD0325901, had striking effects on reducing overall tumor volumes (Figure 2A, 2B). This result was not seen with the REC12 model, which contained a KRAS G12D mutation (Figure 2C). In fact, all single agents had little impact on tumor growth in the REC12 model. It is worth noting that this model was derived from a patient that presented with aggressive disease and experienced relapse within a year of primary therapy. Given the potential effects of constitutive KRAS on both PI3K and mTOR, activation of these pathways was determined by immunohistochemistry (IHC) in vehicle treated animals (Figure 2D-F). As expected, both MAPK and mTOR pathways were highly active as shown by pERK (T202/Y204) and pS6 (S235/236) levels, while PI3K/mTORC2 activity as measured by pAKT (S473) was more moderate. Upregulation of PI3K and/or mTOR pathways, in conjunction with aberrant KRAS signaling, could have made tumors less dependent on any one of these mechanisms for growth. For this reason, both PI3K (BEZ235) and mTOR (AZD8055) single agents were paired with PD0325901 to test the efficacy of combination therapy within this KRAS G12D genetic context. In comparison to single agent treatment, both MEK combination therapies produced heightened tumor responses (Figure 3A). Additionally, this translated into better overall survival, as the control group averaged tumor burdens requiring euthanasia by 14 days following treatment initiation.

To summarize the tumor responses within this study, percent change in tumor volume from initial treatment (day 0) to the end of the study (day 21) was calculated and represented relative to vehicle controls. After three weeks of

Patient-derived xenografts of colorectal cancer

Table 3. Druggable pathway nodes

Druggable Signaling Pathway	Molecular Target (Gene Symbol)	Drug Name (Trade Names)	Company (Highest Trial Phase ^a)
PI3K-AKT Signaling	PIK3CA	BEZ235, BKM120 (Buparlisib), GDC-0941 (Pictilisib), PF-05212384, GDC-0980, GDC-0084, GDC-0032.	Novartis (2), Novartis (3), Genentech/Roche (2), Pfizer (2), Genentech/Roche (2), Genentech/Roche (1), Genentech/Roche (3).
mTOR Signaling	MTOR	AZD8055, RAD001 (Afinitor), Rapamycin (Rapamune), Temozolimus (Torisel), BEZ235, MK8669 (Ridaforolimus).	AstraZeneca (1), Novartis (FDA), Pfizer (FDA), Pfizer (FDA), Novartis (2), Merck (3).
MAPK Signaling	MAP2K1, MAP2K2	PD0325901, Trametinib (Mekinist), GDC-0973 (Cobimetinib), AZD6244 (Selumetinib), MEK162 (ARRY-162), GDC-0623.	Pfizer (2), GlaxoSmithKline (FDA), Genentech/Roche (3), AstraZeneca (3), Novartis (3), Genentech/Roche (1).

^aTrial information reflects review of clinical postings from the NCI and NIH accessed in November 2014. These searches were done at both <http://www.cancer.gov/drugdictionary> and <https://clinicaltrials.gov/> using drug names to identify the most advanced stage of past or current studies.

Table 4. Xenograft dosing schedule

Agent	Dose	Route	Schedule
AZD8055	20 mg/kg	p.o.	QD x 5
BEZ235	40 mg/kg	p.o.	QD x 5
PD0325901	20 mg/kg	p.o.	QD x 5
AZD8055 + PD0325901	20 mg/kg, 20 mg/kg	p.o.	QD x 5
BEZ235 + PD0325901	40 mg/kg (B), 20 mg/kg (P)	p.o.	QD x 5

Abbreviations: p.o., by mouth; QD, daily.

therapy, all single agent therapies reduced tumor burden by approximately 35-40%, while both combined therapies decreased the best single agent response by an additional 25-35% (**Figure 3B**). Next, all collected data was fit to a mixed linear model to account for mouse to mouse variation, which enabled us to determine the statistical significance of differences in tumor volume. Confidence intervals of 95% were subsequently constructed and graphed. While no appreciable differences were observed prior to treatment, all treatment regimens resulted in significant decreases in tumor growth. Both combination therapies significantly decreased tumor volume compared to vehicle controls after only 7 days of treatment (**Figure 3C**). Single agents, BEZ235 and PD0325901,

followed at 9 days, each having equivalent effects on tumor volume until approximately day 14; at this point, BEZ-235-treated tumors exhibited renewed growth, while AZD-8055 treatment did not elicit statistically significant decreases until day 17 (**Figure 3D**). Taken together, these results illustrate the influence of driver

oncogenes on tumor responses to molecularly targeted agents.

REC12 cellular characterization studies

Tumor sections were analyzed by immunohistochemistry for Ki67, a nuclear antigen present in actively proliferating cells. While Ki67 positivity was noted across all groups to varying degrees, proliferation indices were calculated to provide further clarity. The highest levels of proliferation were observed within the vehicle group where nearly 20% of all tumor cells were Ki67 positive (Ki67⁺) (**Figure 4A**). In contrast, all treatment arms showed varying degrees of reduced Ki67 positivity. While tumor volumes reflected a dynamic range between single and

Patient-derived xenografts of colorectal cancer

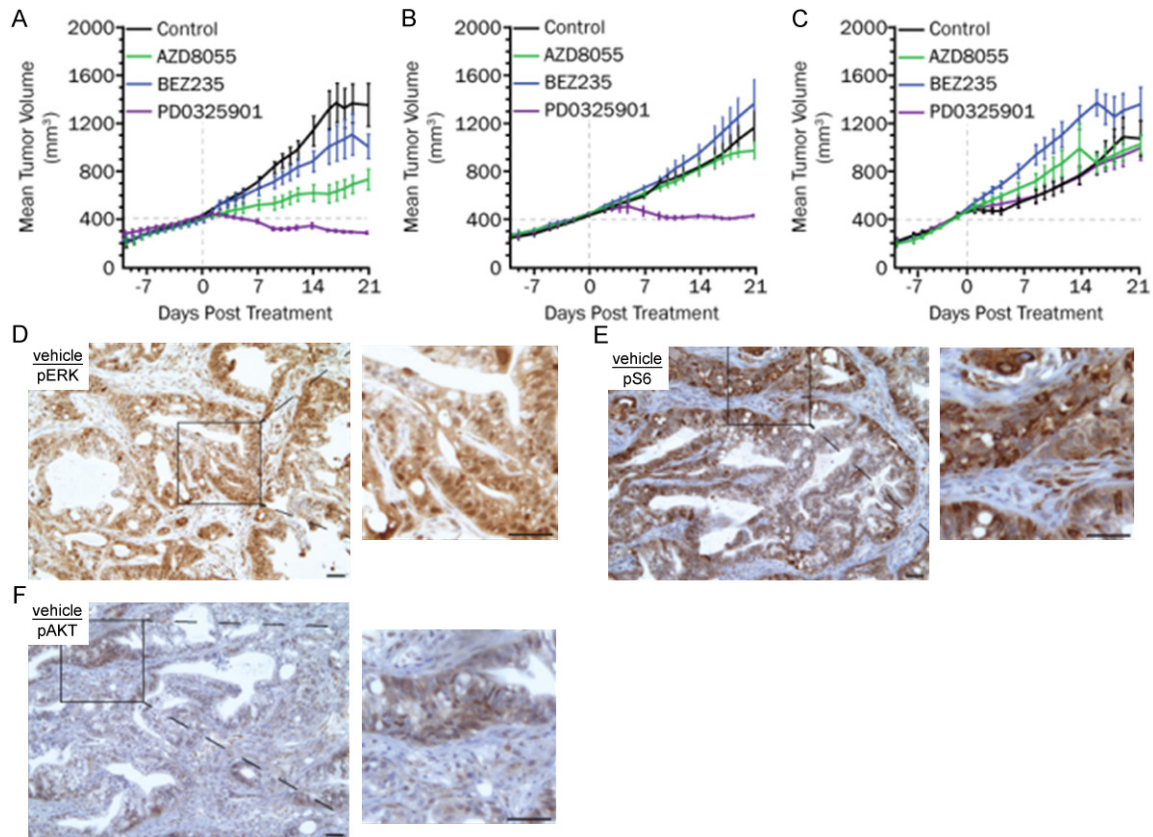


Figure 2. *In vivo* efficacy of molecularly targeted compounds in three PDX models of CRC. (A-C) Three tumors with differing PI3K and RAS mutations were subcutaneously implanted into gender matched athymic nudes. Tumors were measured over time with treatment enrollment occurring randomly once tumor volumes reached 400 mm³. Compounds were administered as delineated in **Table 4**. The models associated with each panel are as follows: (A) COL02, (B) COL18, and (C) REC12. (D-F) At the conclusion of these studies, REC12 tumors from vehicle treated controls were harvested and sections were stained for pERK (D), pS6 (E), and pAKT (F) to determine the extent of MAPK, mTOR, and PI3K signaling within this model.

combination agents, the overall Ki67 proliferation indices were quite comparable. The combination of AZD8055 and PD0325901, or the combination of BEZ235 and PD0325901 showed low proliferative indices at 4.0% and 4.4%, respectively (**Figure 4B, 4C**).

To determine the impact of these compounds on their molecular targets, we assessed activity of PI3K/mTORC2 (pAKT-S473), mTOR (pS6-S240/244), and MAPK (pERK-Y202/204) across all treatment groups. Control treated animals exhibited strong pAKT and pS6 staining within the tumor compartment (**Figure 5A, 5B**, top panel). Positivity was also identified within selective areas of the stroma. In contrast, tumors from combination treatment arms showed overall reductions in abundance and intensity of both pAKT and pS6 (**Figure 5A, 5B**, middle-bottom panels). As expected, individual mTOR (AZD8055) and dual PI3K/mTOR (BE-

Z235) inhibition exhibited more pronounced decreases in pS6 when compared to MEK inhibition (PD0325901). These results were enhanced when mTOR and MEK inhibition were combined. Vehicle treated tumors showed intense pERK-Y202/204 staining within a majority of the tumor bed (**Figure 5C**, top panel). Marked decreases were observed in all treatment groups with BEZ235 + PD0325901 representing the strongest responses (**Figure 5C**, bottom panel). While showing drastic reductions in pERK when compared to vehicle controls, AZD8055 + PD0325901 combination therapy exhibited the lowest effect on this signaling cascade across drug groups (**Figure 5C**, middle panel).

Discussion

The high failure rate of compounds entering clinical trials has illustrated the poor predictive

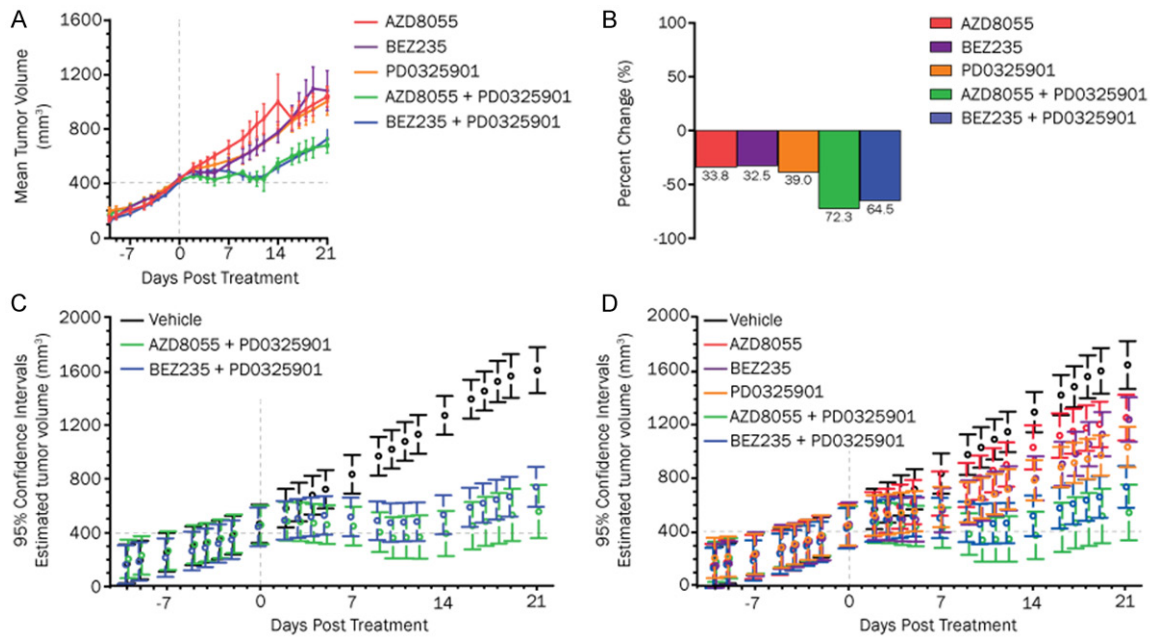


Figure 3. PI3K/mTOR/MEK combination therapy promotes statistically significant reductions in tumor burden. (A) Tumor growth of the REC12 PDX model was plotted to offer specific comparisons between single agents and combination therapies after 21 days. Significance was determined by repeated measures analyses and shown in panels (C and D). (B) Tumor volume averages from each treatment group were calculated at days 0 and 21 and presented as percentages of vehicle. (C, D) 95% confidence intervals for treatment groups were constructed and plotted following fit to a mixed linear model.

power of current preclinical models [8]. Newly developed compounds are often tested in only a small subset of experimental scenarios before entering human trials; thus allowing many unsuitable therapeutics to advance into the most expensive phase of drug development [49]. While cell line xenografts can be easily implemented, strong evidence within the research community shows that these models are insufficient, and often misleading, in the pursuit of new and improved compounds [8, 49]. Because PDX models retain many disease features that are lacking in other models, they have gained momentum as an alternative approach. These improved models preserve intratumor heterogeneity, cell signaling dynamics, and elements of the tumor microenvironment. Therefore, when assessing new therapeutics, PDX models serve an essential role in the preclinical validation process by providing a deeper understanding of effective drug regimens and ultimately maximizing success rates.

With almost 140,000 diagnoses this year alone, CRC remains a substantial clinical problem. Late stage diagnoses continue to have few therapeutic options and poor overall survival. This clearly underscores the need for more

impactful clinical gains within this subset of patients. As with many malignancies, currently available treatment regimens have begun to include molecularly targeted compounds in the hopes of conferring better overall survival while limiting side effects. However, the strength of these therapies also reflects a key shortcoming. In contrast to their systemic cytotoxic counterparts with limited specificity for their antitumor activity, small molecule inhibitors target distinct population(s) of cells that have heightened activity of a given signaling transduction pathway. Presumably this heightened activity represents an axis upon which these cells are dependent for survival. Herein lays their potential value as therapeutic targets. Before these compounds can provide enhanced antitumor effects, genomic characterization of all CRC cases should be conducted to ensure the appropriate subset of patients are being allotted to these treatment regimens. In this study, we first report the establishment and characterization of PDX models that recapitulate both the predominant histological and genomic features of CRC.

To elucidate the utility of these genetically diverse PDX models in preclinical drug evalua-

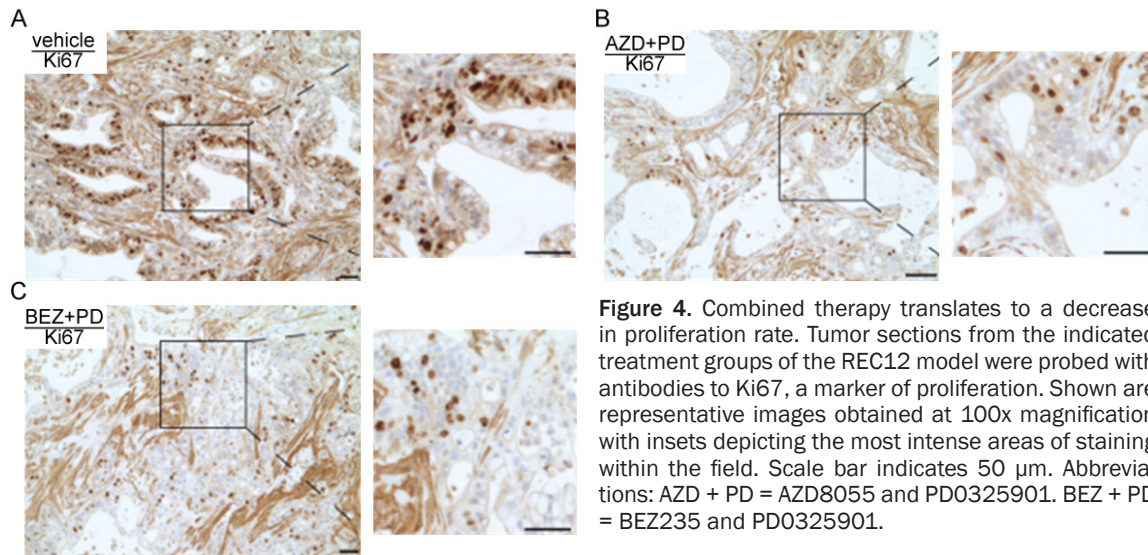


Figure 4. Combined therapy translates to a decrease in proliferation rate. Tumor sections from the indicated treatment groups of the REC12 model were probed with antibodies to Ki67, a marker of proliferation. Shown are representative images obtained at 100x magnification with insets depicting the most intense areas of staining within the field. Scale bar indicates 50 μ m. Abbreviations: AZD + PD = AZD8055 and PD0325901. BEZ + PD = BEZ235 and PD0325901.

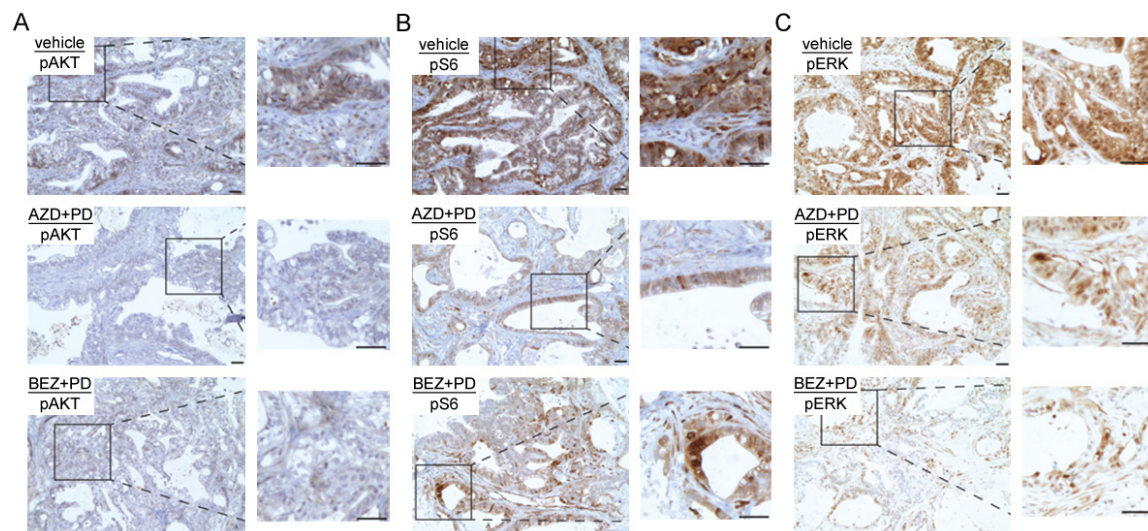


Figure 5. Effects of combined therapy on PI3K/mTOR/MAPK activation. Sections from vehicle and both combination regimens were stained for PI3K (pAKT, left panel), mTOR (pS6, middle panel), and MAPK (pERK, right panel) activation by immunohistochemistry. Scale bars indicate 50 μ m. Abbreviations: AZD + PD = AZD8055 and PD0325901. BEZ + PD = BEZ235 and PD0325901.

tion studies, we filtered for commonly found alterations in human CRC to find most models contained mutations that converged on the PI3K, mTOR, and RAS pathways. Small molecule inhibitors directed against these axes were tested to ascertain potential vulnerabilities that may be clinically actionable within these genetic subgroups of CRC.

Interestingly, MAPK inhibition alone was sufficient to halt tumor growth within just days of treatment initiation. This finding suggests that MAPK signaling may represent a common

mediator of CRC growth within these PDX models. Notably, treatment with the dual PI3K/mTOR inhibitor, BEZ235, had little added benefit than mTOR inhibition alone to suggest more tumor-promoting cues are signaling at the level of mTOR than from upstream signaling components like PI3K.

A single exception to this MAPK sensitivity was noted. Targeting any individual pathway within the REC12 model, which has a KRAS G12D mutation, had only modest effects on tumor growth. Incidentally, this patient, upon review

of medical records, was the first of all patients enrolled in the study to relapse following primary treatment. Like many RAS malignancies, the KRAS^{G12D} model displayed aggressive properties both clinically and *in vivo*. While single agents were relatively ineffective, both combination regimens more than doubled tumor responses. This result does support previously published retrospective studies that suggest different amino acid substitutions at codon 12 can translate to variable sensitivity to both cytotoxic and targeted therapies [50-52]. Taken together, these studies suggest that PDX models with genomic heterogeneity may be valuable models in preclinical drug evaluation particularly in the development of small molecule inhibitors.

To complement the tumor volume measurements, proliferation indices were calculated for each treatment group. As previously cited, tumors with ~15% Ki67-positivity reflect highly proliferative tumors [32-35]. Changes in Ki67⁺ were relatively uniform across all groups; reducing Ki67⁺ down to 3 to 8% from 20% observed in the vehicle group; suggesting all molecularly targeted treatments limited proliferation to similar degrees. Interestingly, we did not observe similar changes in tumor volume across all treatment groups. These discrepancies are likely a reflection of overall tumor composition and timing of Ki67 measurements. Proliferation index calculations use IHC to specifically quantify viable cells within the tumor bed. In contrast, volume measurements reflect the tumor and surrounding microenvironment, which includes varying amounts of stroma and cellular debris. It is plausible that treatments may target important support cells, such as the vascular endothelium or the stroma, rather than directly impacting the tumor bed. With the loss of vasculature, the stromal compartment may expand in an attempt to compensate for lost resources. Whether these compounds act directly upon the tumor bed or target auxiliary cells, they translate to important reductions in functional tumor burden.

In addition to measuring proliferation, IHC was used to confirm pathway inhibition on downstream components. Phospho-substrates AKT, ERK, and S6 had moderate to substantial decreases with a few notable exceptions. AKT was inhibited to varying degrees across all treatment groups with combination treatments

exhibiting the most dramatic responses. This robust decline in PI3K pathway activation can likely be attributed to the ability of catalytic inhibitors BEZ235 and AZD8055 to target both of the molecular complexes in which mTOR exists (mTORC1 and mTORC2). Unlike other rapamycin analogs that exclusively act on TORC1 while leaving TORC2 active to initiate AKT signaling, AZD8055 and BEZ235 inhibit activity of both TORC1 and TORC2. As a result, these two singular therapies elicit similar results as confirmed by the IHC for pAKT (S473), a TORC2 substrate. As expected, the overall effect on pS6 levels was most dramatic with AZD8055 treatment alone and in combination, while all other regimens showed varying degrees of signal. While AZD8055 and BEZ235 target this pathway directly, MAPK signaling can enhance mTOR signaling through TSC2 inactivation [53]. With treatment of the MAPK inhibitor, PD0325901, MAPK-mediated TSC2 inhibition is removed and results in reduced overall mTOR activity.

As this study and others have highlighted, a patient's genetic landscape represents just one important consideration to best showcase the potential benefit of small molecule inhibitor treatment strategies. The PI3K, mTOR, and MAPK pathways are intricately connected, and perturbations of these highly regulated pathways can often influence how cancer cells respond to targeted therapies [54]. While approximately 50% of patients with advanced CRC respond to systemic therapies, virtually all patients eventually progress [55]. The development of molecularly targeted treatment strategies within relevant *in vivo* models will better position clinicians to stratify patients into combination therapies that are tailored to treat genetically distinct CRC cases.

Acknowledgements

Research reported in this article was supported by the Ferguson-Blodgett Digestive Disease Institute, Spectrum Health Medical Group under award numbers (DDI.FY10.01 and DDI.FY10.02) and by Van Andel Research Institute. We acknowledge the patients and their families that agreed to participate in this project. From Spectrum Health, we thank Drs. Anthony Senagore and Heather Slay for their assistance with tumor resection as well as Kim Mohr and Pam Grady for coordinating all clinical annota-

tion and coordination. We also acknowledge Lisa Turner for her assistance with optimization of the IHC assays.

Disclosure of conflict of interest

None.

Address correspondence to: Dr. Jeffrey P MacKeigan, Laboratory of Systems Biology, Van Andel Institute, 333 Bostwick Avenue, Grand Rapids, MI 49503, USA. Tel: 616 234-5682; E-mail: jeff.mackeigan@vai.org

References

- [1] Kola I, Landis J. Can the pharmaceutical industry reduce attrition rates? *Nat Rev Drug Discov* 2004; 3: 711-715.
- [2] Sausville EA, Burger AM. Contributions of human tumor xenografts to anticancer drug development. *Cancer Res* 2006; 66: 3351-3354; discussion 3354.
- [3] Daniel VC, Marchionni L, Hierman JS, Rhodes JT, Devereux WL, Rudin CM, Yung R, Parmigiani G, Dorsch M, Peacock CD, Watkins DN. A primary xenograft model of small-cell lung cancer reveals irreversible changes in gene expression imposed by culture in vitro. *Cancer Res* 2009; 69: 3364-3373.
- [4] Pampaloni F, Reynaud EG, Stelzer EH. The third dimension bridges the gap between cell culture and live tissue. *Nat Rev Mol Cell Biol* 2007; 8: 839-845.
- [5] Talmadge JE, Singh RK, Fidler IJ, Raz A. Murine models to evaluate novel and conventional therapeutic strategies for cancer. *Am J Pathol* 2007; 170: 793-804.
- [6] Rubio-Viqueira B, Hidalgo M. Direct in vivo xenograft tumor model for predicting chemotherapeutic drug response in cancer patients. *Clin Pharmacol Ther* 2009; 85: 217-221.
- [7] Williams SA, Anderson WC, Santaguida MT, Dylla SJ. Patient-derived xenografts, the cancer stem cell paradigm, and cancer pathobiology in the 21st century. *Lab Invest* 2013; 93: 970-982.
- [8] Siolas D, Hannon GJ. Patient-derived tumor xenografts. Transforming clinical samples into mouse models. *Cancer Res* 2013; 73: 5315-5319.
- [9] Houghton PJ, Morton CL, Tucker C, Payne D, Favours E, Cole C, Gorlick R, Kolb EA, Zhang W, Lock R, Carol H, Tajbakhsh M, Reynolds CP, Maris JM, Courtright J, Keir ST, Friedman HS, Stopford C, Zeidner J, Wu J, Liu T, Billups CA, Khan J, Ansher S, Zhang J, Smith MA. The pediatric preclinical testing program: description of models and early testing results. *Pediatr Blood Cancer* 2007; 49: 928-940.
- [10] Hidalgo M, Bruckheimer E, Rajeshkumar NV, Garrido-Laguna I, De Oliveira E, Rubio-Viqueira B, Strawn S, Wick MJ, Martell J, Sidransky D. A pilot clinical study of treatment guided by personalized tumorgrafts in patients with advanced cancer. *Mol Cancer Ther* 2011; 10: 1311-1316.
- [11] Begley CG, Ellis LM. Drug development. Raise standards for preclinical cancer research. *Nature* 2012; 483: 531-533.
- [12] Siegel R, Desantis C, Jemal A. Colorectal cancer statistics, 2014. *CA Cancer J Clin* 2014; 64: 104-117.
- [13] Society AC. Colorectal Cancer Facts & Figures 2011-2013. Atlanta: American Cancer Society; 2011. pp. 1-32.
- [14] Scott AM, Wolchok JD, Old LJ. Antibody therapy of cancer. *Nat Rev Cancer* 2012; 12: 278-287.
- [15] Hoda D, Simon GR, Garrett CR. Targeting colorectal cancer with anti-epidermal growth factor receptor antibodies. focus on panitumumab. *Ther Clin Risk Manag* 2008; 4: 1221-1227.
- [16] Saif MW. Anti-VEGF agents in metastatic colorectal cancer (mCRC). are they all alike? *Cancer Manag Res* 2013; 5: 103-115.
- [17] Brand TM, Wheeler DL. KRAS mutant colorectal tumors. past and present. *Small GTPases* 2012; 3: 34-39.
- [18] Lievre A, Bachet JB, Boige V, Cayre A, Le Corre D, Buc E, Ychou M, Bouche O, Landi B, Louvet C, André T, Bibeau F, Diebold MD, Rougier P, Ducreux M, Tomasic G, Emile JF, Penault-Llorca F, Laurent-Puig P. KRAS mutations as an independent prognostic factor in patients with advanced colorectal cancer treated with cetuximab. *J Clin Oncol* 2008; 26: 374-379.
- [19] Lievre A, Bachet JB, Le Corre D, Boige V, Landi B, Emile JF, Cote JF, Tomasic G, Penna C, Ducreux M, Rougier P, Penault-Llorca F, Laurent-Puig P. KRAS mutation status is predictive of response to cetuximab therapy in colorectal cancer. *Cancer Res* 2006; 66: 3992-3995.
- [20] Lievre A, Laurent-Puig P. Genetics: Predictive value of KRAS mutations in chemoresistant CRC. *Nat Rev Clin Oncol* 2009; 6: 306-307.
- [21] Bos JL. The ras gene family and human carcinogenesis. *Mutat Res* 1988; 195: 255-271.
- [22] Wennerberg K, Rossman KL, Der CJ. The Ras superfamily at a glance. *J Cell Sci* 2005; 118: 843-846.
- [23] Cox AD, Der CJ. Ras family signaling. therapeutic targeting. *Cancer Biol Ther* 2002; 1: 599-606.
- [24] Bollag G, McCormick F. Regulators and effectors of ras proteins. *Annu Rev Cell Biol* 1991; 7: 601-632.

- [25] Verdine GL, Walensky LD. The challenge of drugging undruggable targets in cancer: lessons learned from targeting BCL-2 family members. *Clin Cancer Res* 2007; 13: 7264-7270.
- [26] Rodon J, Dienstmann R, Serra V, Tabernero J. Development of PI3K inhibitors: lessons learned from early clinical trials. *Nat Rev Clin Oncol* 2013; 10: 143-153.
- [27] Santarpia L, Lippman SM, El-Naggar AK. Targeting the MAPK-RAS-RAF signaling pathway in cancer therapy. *Expert Opin Ther Targets* 2012; 16: 103-119.
- [28] Hoefflich KP, O'Brien C, Boyd Z, Cavet G, Guerrero S, Jung K, Januario T, Savage H, Punnoose E, Truong T, Zhou W, Berry L, Murray L, Amler L, Belvin M, Friedman LS, Lackner MR. In vivo antitumor activity of MEK and phosphatidylinositol 3-kinase inhibitors in basal-like breast cancer models. *Clin Cancer Res* 2009; 15: 4649-4664.
- [29] Kinross KM, Brown DV, Kleinschmidt M, Jackson S, Christensen J, Cullinane C, Hicks RJ, Johnstone RW, McArthur GA. In vivo activity of combined PI3K/mTOR and MEK inhibition in a Kras(G12D);Pten deletion mouse model of ovarian cancer. *Mol Cancer Ther* 2011; 10: 1440-1449.
- [30] Engelman JA, Chen L, Tan X, Crosby K, Guimaraes AR, Upadhyay R, Maira M, McNamara K, Perera SA, Song Y, Chirieac LR, Kaur R, Lightbown A, Simendinger J, Li T, Padera RF, García-Echeverría C, Weissleder R, Mahmood U, Cantley LC, Wong KK. Effective use of PI3K and MEK inhibitors to treat mutant Kras G12D and PIK3CA H1047R murine lung cancers. *Nat Med* 2008; 14: 1351-1356.
- [31] Willems L, Chapuis N, Puissant A, Maciel TT, Green AS, Jacque N, Vignon C, Park S, Guichard S, Herault O, Fricot A, Hermine O, Moura IC, Auberger P, Ifrah N, Dreyfus F, Bonnet D, Lacombe C, Mayeux P, Bouscary D, Tamburini J. The dual mTORC1 and mTORC2 inhibitor AZD8055 has anti-tumor activity in acute myeloid leukemia. *Leukemia* 2012; 26: 1195-1202.
- [32] Chresta CM, Davies BR, Hickson I, Harding T, Cosulich S, Critchlow SE, Vincent JP, Ellston R, Jones D, Sini P, James D, Howard Z, Dudley P, Hughes G, Smith L, Maguire S, Hummersone M, Malagu K, Menear K, Jenkins R, Jacobsen M, Smith GC, Guichard S, Pass M. AZD8055 is a potent, selective, and orally bioavailable ATP-competitive mammalian target of rapamycin kinase inhibitor with in vitro and in vivo antitumor activity. *Cancer Res* 2010; 70: 288-298.
- [33] Renshaw J, Taylor KR, Bishop R, Valenti M, De Haven Brandon A, Gowan S, Eccles SA, Ruddle RR, Johnson LD, Raynaud FI, Selfe JL, Thway K, Pietsch T, Pearson AD, Shipley J. Dual Blockade of the PI3K/AKT/mTOR (AZD8055) and RAS/MEK/ERK (AZD6244) Pathways Synergistically Inhibits Rhabdomyosarcoma Cell Growth In Vitro and In Vivo. *Clin Cancer Res* 2013; 19: 5940-51.
- [34] Nyfeler B, Chen Y, Li X, Pinzon-Ortiz M, Wang Z, Reddy A, Pradhan E, Das R, Lehár J, Schlegel R, Finan PM, Cao ZA, Murphy LO, Huang A. RAD001 enhances the potency of BEZ235 to inhibit mTOR signaling and tumor growth. *PLoS One* 2012; 7: e48548.
- [35] Maira SM, Stauffer F, Brueggen J, Furet P, Schnell C, Fritsch C, Brachmann S, Chène P, De Pover A, Schoemaker K, Fabbro D, Gabriel D, Simonen M, Murphy L, Finan P, Sellers W, García-Echeverría C. Identification and characterization of NVP-BEZ235, a new orally available dual phosphatidylinositol 3-kinase/mammalian target of rapamycin inhibitor with potent in vivo antitumor activity. *Mol Cancer Ther* 2008; 7: 1851-1863.
- [36] Haagensen EJ, Kyle S, Beale GS, Maxwell RJ, Newell DR. The synergistic interaction of MEK and PI3K inhibitors is modulated by mTOR inhibition. *Br J Cancer* 2012; 106: 1386-1394.
- [37] Kirstein MM, Boukouris AE, Pothiraju D, Buitrago-Molina LE, Marhenke S, Schutt J, Orlik J, Kuhnle F, Hegermann J, Manns MP, Vogel A. Activity of the mTOR inhibitor RAD001, the dual mTOR and PI3-kinase inhibitor BEZ235 and the PI3-kinase inhibitor BKM120 in hepatocellular carcinoma. *Liver Int* 2013; 33: 780-793.
- [38] Venkannagari S, Fiskus W, Peth K, Atadja P, Hidalgo M, Maitra A, Bhalla KN. Superior efficacy of co-treatment with dual PI3K/mTOR inhibitor NVP-BEZ235 and pan-histone deacetylase inhibitor against human pancreatic cancer. *Oncotarget* 2012; 3: 1416-1427.
- [39] Liu TJ, Koul D, LaFortune T, Tiao N, Shen RJ, Maira SM, Garcia-Echeverria C, Yung WK. NVP-BEZ235, a novel dual phosphatidylinositol 3-kinase/mammalian target of rapamycin inhibitor, elicits multifaceted antitumor activities in human gliomas. *Mol Cancer Ther* 2009; 8: 2204-2210.
- [40] Cho DC, Cohen MB, Panka DJ, Collins M, Ghebremichael M, Atkins MB, Signoretti S, Mier JW. The efficacy of the novel dual PI3-kinase/mTOR inhibitor NVP-BEZ235 compared with rapamycin in renal cell carcinoma. *Clinical cancer research*. *Clin Cancer Res* 2010; 16: 3628-3638.
- [41] Eichhorn PJ, Gili M, Scaltriti M, Serra V, Guzman M, Nijkamp W, Beijersbergen RL, Valero V, Seoane J, Bernards R, Baselga J. Phosphatidylinositol 3-kinase hyperactivation results in lapatinib resistance that is reversed by the mTOR/phosphatidylinositol 3-kinase inhibitor

- NVP-BEZ235. *Cancer Res* 2008; 68: 9221-9230.
- [42] Hofmann I, Weiss A, Elain G, Schwaederle M, Sterker D, Romanet V, Schmelzle T, Lai A, Brachmann SM, Bentires-Alj M, Roberts TM, Sellers WR, Hofmann F, Maira SM. K-RAS mutant pancreatic tumors show higher sensitivity to MEK than to PI3K inhibition in vivo. *PLoS One* 2012; 7: e44146.
- [43] Sebolt-Leopold JS, Herrera R. Targeting the mitogen-activated protein kinase cascade to treat cancer. *Nat Rev Cancer* 2004; 4: 937-947.
- [44] Fearon ER. Molecular genetics of colorectal cancer. *Annu Rev Pathol* 2011; 6: 479-507.
- [45] Houghton PJ, Gorlick R, Kolb EA, Lock R, Carol H, Morton CL, Keir ST, Reynolds CP, Kang MH, Phelps D, Maris JM, Billups C, Smith MA. Initial testing (stage 1) of the mTOR kinase inhibitor AZD8055 by the pediatric preclinical testing program. *Pediatric Blood Cancer* 2012; 58: 191-199.
- [46] Hennig M, Yip-Schneider MT, Wentz S, Wu H, Hekmatyar SK, Klein P, Bansal N, Schmidt CM. Targeting mitogen-activated protein kinase kinase with the inhibitor PD0325901 decreases hepatocellular carcinoma growth in vitro and in mouse model systems. *Hepatology* 2010; 51: 1218-1225.
- [47] Henderson YC, Chen Y, Frederick MJ, Lai SY, Clayman GL. MEK inhibitor PD0325901 significantly reduces the growth of papillary thyroid carcinoma cells in vitro and in vivo. *Molr Cancer Ther* 2010; 9: 1968-1976.
- [48] Yasumizu Y, Miyajima A, Kosaka T, Miyazaki Y, Kikuchi E, Oya M. Dual PI3K/mTOR Inhibitor NVP-BEZ235 Sensitizes Docetaxel in Castration Resistant Prostate Cancer. *J Urol* 2013; 191: 227-34.
- [49] Monsma DJ, Monks NR, Cherba DM, Dylewski D, Eugster E, Jahn H, Srikanth S, Scott SB, Richardson PJ, Everts RE, Ishkin A, Nikolsky Y, Resau JH, Sigler R, Nickoloff BJ, Webb CP. Genomic characterization of explant tumor-graft models derived from fresh patient tumor tissue. *J Transl Med* 2012; 10: 125.
- [50] De Roock W, Jonker DJ, Di Nicolantonio F, Sartore-Bianchi A, Tu D, Siena S, Lamba S, Arena S, Frattini M, Piessevaux H, Van Cutsem E, O'Callaghan CJ, Khambata-Ford S, Zalcberg JR, Simes J, Karapetis CS, Bardelli A, Tejpar S. Association of KRAS p.G13D mutation with outcome in patients with chemotherapy-refractory metastatic colorectal cancer treated with cetuximab. *JAMA* 2010; 304: 1812-1820.
- [51] Tejpar S, Celik I, Schlichting M, Sartorius U, Bokemeyer C, Van Cutsem E. Association of KRAS G13D tumor mutations with outcome in patients with metastatic colorectal cancer treated with first-line chemotherapy with or without cetuximab. *J Clin Oncol* 2012; 30: 3570-3577.
- [52] Tan C, Du X. KRAS mutation testing in metastatic colorectal cancer. *World J Gastroenterol* 2012; 18: 5171-5180.
- [53] Ma L, Chen Z, Erdjument-Bromage H, Tempst P, Pandolfi PP. Phosphorylation and functional inactivation of TSC2 by Erk implications for tuberous sclerosis and cancer pathogenesis. *Cell* 2005; 121: 179-193.
- [54] Wee S, Jagani Z, Xiang KX, Loo A, Dorsch M, Yao YM, Sellers WR, Lengauer C, Stegmeier F. PI3K pathway activation mediates resistance to MEK inhibitors in KRAS mutant cancers. *Cancer Res* 2009; 69: 4286-4293.
- [55] Dallas NA, Xia L, Fan F, Gray MJ, Gaur P, van Buren G 2nd, Samuel S, Kim MP, Lim SJ, Ellis LM. Chemoresistant colorectal cancer cells, the cancer stem cell phenotype, and increased sensitivity to insulin-like growth factor-I receptor inhibition. *Cancer Res* 2009; 69: 1951-1957.